Glycerol as Reaction Medium for Sonogashira Couplings: A Green Approach for the Synthesis of New Triarylamine-Based Materials with Potential Application in Optoelectronics

Venanzio Raglione,[a] Federica Palmeri,[a, b] Giuseppe Mattioli,[a] Francesco Porcelli,[a] Daniela Caschera,[c] and Gloria Zanotti*[a]

This study focuses on the design, eco-friendly synthesis, and characterization of several novel three-legged triphenylamine derivatives. By performing Sonogashira couplings of functionalized aryl iodides with tris(4-ethynylphenyl)amine in glycerol, a readily available bio-derived solvent, we achieved the synthesis of target products in short times and high yields, up to 94%, with consistently lower E-factors and reduced costs compared to standard conditions using toluene as the reaction medium.

The target molecules possess a D-(π-A)$_3$ or D-(π-D)$_3$ structure, where an electron-donating core connects to three electron-donating (D) or electron-accepting (A) peripheral aromatic subunits through an acetylene spacer. Their main optical and electronic properties have been determined experimentally and by DFT simulations and suggest a possible implementation in energy conversion technologies such as luminescent solar concentrators (LSCs) and perovskite solar cells (PSCs).

Introduction

The field of chemistry plays a crucial role in our everyday lives, providing materials for everything from medicine to electronics and clothing. However, traditional synthetic methods often rely on harsh chemicals, generate hazardous waste and require high energy consumption. This raises a critical question: can we achieve the advancements we desire without sacrificing the environment? The answer is in the rapidly evolving approaches of sustainable synthesis, which prioritize minimizing the environmental impact of chemical reactions.[1] This translates to developing methods that are environmentally friendly, resource efficient, and energy conscious. Such approaches involve the use of less harmful or non-toxic chemicals, bio-derived reagents, and readily biodegradable or recyclable solvents.[2] Resource efficiency comes from minimizing waste generation through

optimizing reaction yields and employing techniques like pot-economical reactions.[3] Finally, energy consciousness harnesses greener heating methods like microwave irradiation or renewable energy sources to power reactions.[4] By minimizing hazardous waste and utilizing safer alternatives, we protect our ecosystems and human health. Efficient processes that use less energy and resources contribute to a more sustainable future. Replacing expensive and hazardous chemicals with greener alternatives can lead to lower production costs in the long run. We believe that sustainable synthesis is not just a trend, but it is a fundamental shift. By embracing greener methods and continually innovating, we can ensure a future where progress and environmental responsibility go hand-in-hand.

Sustainable synthesis holds immense potential for the field of organic π-conjugated systems, which are attracting significant interest for their remarkable optoelectronic properties.[5] By manipulating the arrangement of donor (D), conjugated transport bridge (π), and acceptor (A) components of the chosen materials, we can create conjugated systems with diverse processability, shapes and features, making them ideal organic semiconductors for transistors,[6] emitting species for organic light emitting diodes (OLEDs),[7] absorbing species for organic photovoltaic (OPV)[8] and charge-transporting materials for emerging organic and hybrid photovoltaic technologies.[9] Among the numerous classes of molecules developed for these purposes, triarylamines possess intriguing features that make them highly studied. Their tripodal structure can be symmetrically or asymmetrically functionalized to produce derivatives with specific optical and electronic properties. Due to this outstanding tunability, triarylamines are extensively studied in cutting-edge technologies, such as perovskite-based photovoltaics.[10]

Furthermore, their intrinsically non-planar structure suppresses intermolecular packing, thereby improving solid emis-

[a] V. Raglione, F. Palmeri, G. Mattioli, F. Porcelli, G. Zanotti
Istituto di Struttura della Materia (ISM), Consiglio Nazionale delle Ricerche (CNR), Strada provinciale 35d/9, Montelibretti 00010, Italy
E-mail: gloria.zanotti@ism.cnr.it

[b] F. Palmeri
Department of Chemistry, Sapienza University of Rome, Piazzale Aldo Moro, 5, Rome 00185, Italy

[c] D. Caschera
Istituto per lo Studio dei Materiali Nanostrutturati (ISMN), Consiglio Nazionale delle Ricerche (CNR), Strada provinciale 35d/9, Montelibretti 00010, Italy

Chemistry–A European Journal

Research Article
doi.org/10.1002/chem.202402901

Chemistry
Europe
European Chemical
Societies Publishing

sion efficiency, making them ideal candidates for implementation in solid-state optoelectronic devices.[11] Nevertheless, while offering good performance and consistency, their traditional synthesis mainly relies on outdated processes that use hazardous and expensive chemicals. Sustainable synthesis offers a solution to this challenge by developing cleaner and more streamlined methods for producing these materials.[12] In the vast realm of carbon-carbon bond formation, the Sonogashira coupling stands out as the most important and widely acknowledged method for forming $C(sp^2)$–$C(sp)$ bonds, with significant relevance to the pharmaceutical industry. Traditionally, palladium complexes combined with copper(I) salts are the preferred catalysts for such reactions, and solvents like acetonitrile (MeCN), tetrahydrofuran (THF), and toluene (Tol) are commonly used. However, these solvents pose environmental and safety issues. Over the years, modifications to the standard procedure have been made to align the process with green chemistry principles by developing copper-free approaches[13] and selecting low-impact solvents like water as the reaction medium,[14] or a combination of the two,[15] as well as employing micellar systems.[16] Solvents, usually used in large excess relative to reactants, can significantly impact the environmental footprint of a synthesis. If a solvent is flammable, toxic, or harmful, it is crucial to find more sustainable and safer alternatives that at the same time preserve the yields of the target reaction. Glycerol, a non-toxic and readily available byproduct of biodiesel production, is emerging as a valuable resource for sustainable organic synthesis.[17] Beyond its role as a solvent, its unique structure with multiple hydroxyl groups allows for participation in a highly interconnected network of hydrogen bonding, potentially influencing reaction rates and selectivity in various organic transformations.[18] Research suggests that glycerol can act as more than just a solvent, potentially improving reaction outcomes in the synthesis of complex molecules.[19] Additionally, its high boiling point and miscibility with water facilitate its recovery and reuse in subsequent reactions, minimizing waste and promoting environmentally friendly practices. The main physical properties of glycerol, along with its structure, are provided in Table 1.

Overall, glycerol presents a compelling alternative to traditional organic solvents, offering a greener and potentially more efficient approach to organic synthesis. It also highlights its potential in the sustainable development of high-value derivatives like hole-transport materials (HTMs) and luminophores. To the best of our knowledge, the use of glycerol as a solvent in Sonogashira reactions appears to be an underexplored area in the literature, with documented success when employed in deep-eutectic solvents[20] and mixtures with *tert*-butanol.[21] In contrast, glycerol has been more extensively applied in other Pd-catalyzed cross-coupling reactions, such as Heck and Suzuki
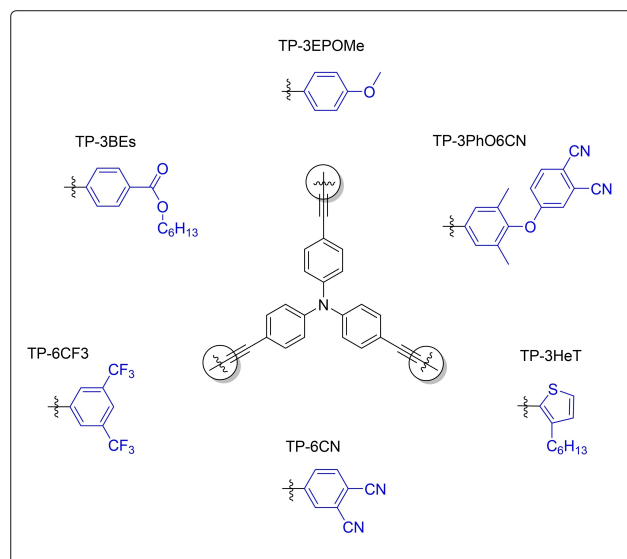
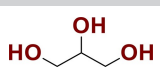**Figure 1.** Structural arrangements of triarylamine derivatives synthesized in this work.

couplings.[18,22] In this work, we present an alternative approach for Sonogashira reactions, replacing conventional media with glycerol, for the synthesis of the novel D-(π-A)₃ and D-(π-D)₃ triarylamine-based derivatives sketched in Figure 1, starting from tris(4-ethynylphenyl)amine and several electron-rich and electron-poor aryl iodides. The functional groups nature and position on the precursors were chosen to evaluate the influence of the electronic nature of the substituents on both the reaction efficiency and the optoelectronic properties of the resulting products. The procedure we developed demonstrated good tolerance to different functional groups, leading to the synthesis of all derivatives in high yield and lower Environmental factor values (E-factors) and estimated costs with respect to control reactions performed in toluene.
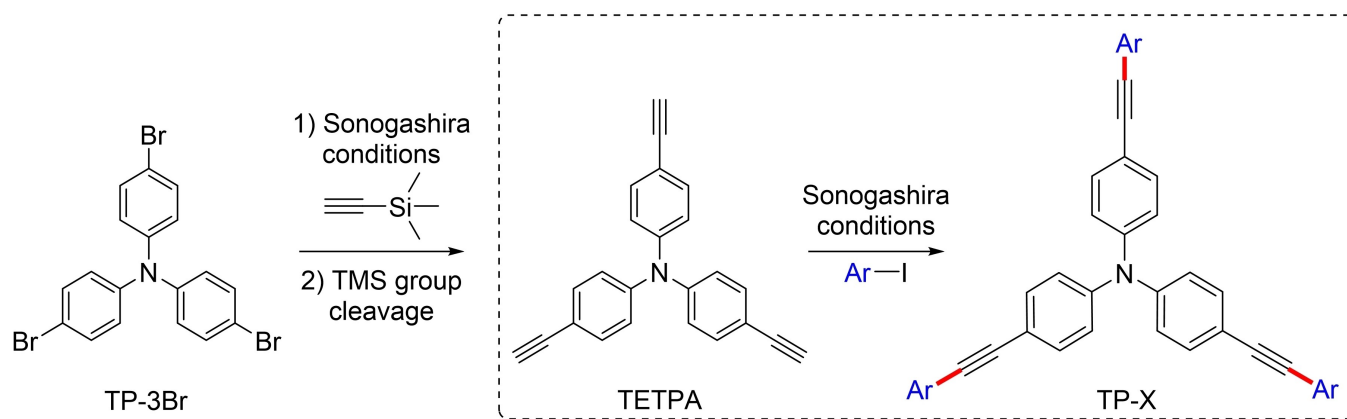
The optical, photo- and electrochemical characterization of our derivatives has revealed a significant dependence of their properties on the nature of the substituents, in good agreement with theoretical calculations. This variability makes the portfolio of synthesized molecules potentially useful in a range of advanced technologies, including next-generation photovoltaics and luminescent solar concentrators.

Results and Discussion

A two-step Sonogashira cross-coupling strategy was employed for the synthesis of target molecules drawn in Figure 1, as outlined in Scheme 1. Tris(4-ethynylphenyl)amine (TETPA)

Table 1. Structure and relevant physical properties of glycerol.					
HO⌒OH, OH glycerol, propane-1,2,3-triol	Molecular Formula	Density [g/mL]	Dipole moment [D]	mp [°C]	bp [°C]
	$C_3H_8O_3$	1.261	2.56	17.8	290

Chem. Eur. J. **2024**, e202402901 (2 of 10)

© 2024 The Author(s). Chemistry - A European Journal published by Wiley-VCH GmbH

Chemistry–A European Journal

Research Article
doi.org/10.1002/chem.202402901

Chemistry
Europe
European Chemical
Societies Publishing

Scheme 1. Synthetic strategy for target molecules starting from tris(4-bromophenyl)amine.

served as the common starting material, prepared from commercially available tris(4-bromophenyl)amine (TP-3Br) via a slightly modification of reported procedures.[23] Subsequent cross-coupling reactions were performed in glycerol between TETPA and several aryl iodides bearing electron-donating or electron-withdrawing groups, namely 4-iodoanisole (TP-3EPOMe), 4-(4-iodo-2,6-dimethylphenoxy)phthalonitrile (TP-3PhO6CN), hexyl 4-iodobenzoate (TP-3BEs), 1-iodo-3,5(bistrifluoromethyl)benzene (TP-6CF3), and 4-iodophthalonitrile (TP-6CN). The reactions were also performed in toluene as a reference solvent for comparison. Tetrakis(triphenylphosphine)palladium(0)/copper(I) iodide [Pd-(PPh$_3$)$_4$/CuI] catalytic system and triethylamine (Et$_3$N) as the base were chosen for both the reaction media. The results, summarized in Table 2, show generally high yields, in accordance with the generally good reactivity of aryl iodides in Sonogashira conditions. Under standard conditions, Sonogashira coupling reactions generally delivered high yields, ranging from 87 to 98%, within 4 to 24 hours. Replacing toluene with glycerol also successfully provided all the target derivatives in good yields, even exceeding those obtained under standard conditions in some cases. This reaction medium proved to be highly advantageous for product isolation, as it precipitates as a solid increasing the rate of reagent disappearance, monitored by TLC, and allowing the reactions to go to completion within

minutes. Given this attractive outcome, attempts were made using triethylamine as the only reaction medium. However, these resulted in a drastic decrease of reaction yields due to the very low solubility of the precursors in it, thus underscoring the necessity of glycerol for achieving successful reactions. The chosen experimental conditions proved tolerant to the variety of functional groups on aryl iodides, demonstrating the versatility of the method. According to the accepted mechanism of the Sonogashira reaction,[24] in the case of the D-(π-A)$_3$ derivatives TP-6CF3 and TP-6CN, the presence of electron-withdrawing substituents on the aryl halide promotes the oxidative addition of the aryl moiety to the Pd(0) catalyst,[25] by reducing the electron density on the C–I bond. Concurrently, electron-donating groups on TP-3EPOMe and TP-3PhO6CN could favor the reductive elimination step.[26] Thus, in the case of the former, the presence of the -OMe group in the para position appears to have a positive influence on the reaction yield, as observed for the TP-6CF3 and TP-6CN derivatives, with -CF$_3$ groups in the meta position and -CN groups in the para and meta positions, respectively. The latter, which bears a "phenol-like" substituent in the *para* position as well as two methyl groups in the *meta* positions also exhibits a similar effect in activating the C–I bond. Surprisingly, TP-3BEs showed a marked decrease in reaction yield when glycerol was used, despite the electron-accepting nature of the hexyl benzoate

Table 2. Yield, E-factor and cost estimation comparisons of the Sonogashira couplings of aryl iodides and bromides with TETPA in conventional solvents and glycerol.

	Compound	Yield (%) Toluene[a]	Yield (%) Glycerol[b]	E-factor Toluene[a]	E-factor Glycerol[b]	Cost (EUR/g) Toluene[a]	Cost (EUR/g) Glycerol[b]
Aryl iodides	TP-3EPOMe	96	87	624.5	393.3	29.90	28.62
	TP-3PhO6CN	89	91	754.7	566.7	66.44	62.22
	TP-3BEs	87	50	628.9	316.4	31.33	38.49
	TP-6CF3	98	89	507.1	271.1	30.00	21.19
	TP-6CN	90	94	765.8	326.8	173.94	159.90
Aryl bromides	TP-3TMSA	93[c]	40	59.0[c]	479.6	10.04[c]	22.31
	TP-3HeT	35	42	2122.7	950.4	109.31	76.39

[a] Aryl halide (3.2 eq), toluene (2 mL), triethylamine (3 mL), Pd(PPh$_3$)$_4$ (0.05 eq), tris(4-ethynylphenyl)amine (1 eq), CuI (0.05 eq). [b] aryl halide (3.2 eq), glycerol (2 mL), triethylamine (3 mL), Pd(PPh$_3$)$_4$ (0.05 eq), tris(4-ethynylphenyl)amine (1 eq), CuI (0.05 eq). [c] Solvent: tetrahydrofuran.

group. This unexpected result prompted further investigation, leading to additional experiments under varying conditions, as summarized in Table 3, to elucidate the underlying cause.

Our findings reveal that yields in glycerol exhibit limited dependence on temperature, with values of 41% at room temperature and 50% at 80°C, reflecting only a 22% relative increase. Substituting, instead, Pd(PPh$_3$)$_4$ with the more commonly used bis(triphenylphosphine)palladium dichloride (Pd-(PPh$_3$)$_2$Cl$_2$) resulted in lower yields under the same conditions. We therefore conclude that the yields are primarily influenced by the chemical nature of the reaction medium, rather than the temperature and the catalyst. Specifically, the nonpolar linear C6 chain of the hexyl 4-iodobenzoate precursor likely contributes to the reduced reactivity in the protic polar solvent glycerol. To test this hypothesis, experiments were conducted using analogous solvents with a C3 chain and fewer hydroxyl groups, such as 1-propanol and propane-1,2-diol. Surprisingly, the reaction in the latter gave a high yield (72%) even at room temperature, while the former provided a modest 34% result. This further puzzling evidence prompted us to consider the different properties of the three C3-based solvents. A plausible explanation could involve the dipole moment of propane-1,2-diol (2.27 D), which is intermediate between those of glycerol (2.56 D) and 1-propanol (1.65 D), as well as its density and viscosity (1.036 g/mL and 0.042 Pa·s respectively). These factors may represent an optimal balance between facilitating the coupling reaction by promoting the dissolution of the iodinated precursor and maintaining a suitable reaction environment. In fact, the solubilization of hexyl-4-iodobenzoate or the related reaction intermediates in glycerol may be suboptimal due to unfavorable interactions between the apolar linear chain and the solvent. Conversely, the presence of only one hydroxyl group on 1-propanol may not efficiently promote the reaction through poor coordination with the aryl iodide. As further proof that the hexyl chain of hexyl-4-iodobenzoate is detrimental to its reactivity in glycerol, a control reaction was performed using methyl-4-iodobenzoate under the same conditions and the target product was synthesized in almost quantitative yield (Scheme 2).
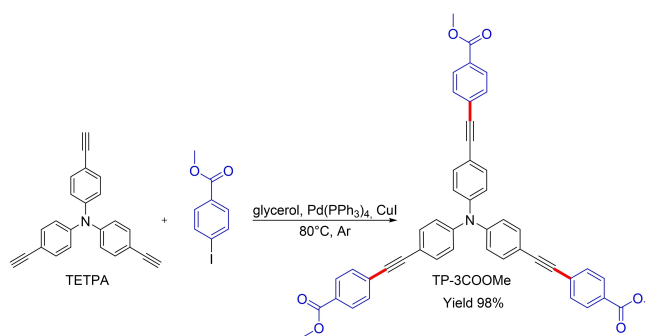
**Scheme 2.** Control reaction between TETPA and methyl-4-iodobenzoate in glycerol.

We calculated the E-factor values of our syntheses, reported in Table 2, and found a significant decrease for all the glycerol procedures compared to those obtained when toluene was used as the solvent, indicating that the isolation and purification of the target products are less resource-intensive in the former. The lowest E-factor value calculated under glycerol conditions was obtained for the TP-6CF3 derivative (E-factor = 271.1), with a difference of 236 compared to the value calculated for the procedure in toluene. This is due to the fact that the crude product in glycerol resulted to be cleaner compared to that obtained under standard conditions, so it was possible to use recrystallization as a purification method employing a smaller quantity of solvent and material, avoiding the use of silica gel. The same observation was made also in the case of the TP-6CN derivative, in which the difference between the E-factor of the standard procedure and that of the glycerol procedure is even more pronounced (ΔE-factor = 439), concurrently with an increase of the reaction yield, further reinforcing the advantage of our approach. This reduction in resource usage is also reflected in the estimated production costs, calculated according to the guidelines proposed by Osedach et al.[27] Additionally, we highlight that these syntheses were performed on a small scale, with batches of 50 mg of the limiting reagent. Scaling up typically enhances sustainability by reducing the volumes of solvents used, suggesting that the

Table 3. Exploration of other solvents and conditions for the synthesis of TP-3BEs.					
Solvent	catalytic system[b]	T [°C]	t [h]	Work up and purification method	Yield [%]
Toluene[a]	Pd(PPh$_3$)$_4$/CuI	80	0.5 to 24	Extraction with DCM Chromatography on silica gel	87
Glycerol[a]	Pd(PPh$_3$)$_4$/CuI	80	0.25 to 24	Filtered on Büchner Recrystallization	50
Glycerol	Pd(PPh$_3$)$_2$Cl$_2$/CuI	25	24	Filtered on Büchner Chromatography on silica gel	34
Glycerol	Pd(PPh$_3$)$_4$/CuI	25	4	Filtered on Büchner Chromatography on silica gel	41
1-propanol	Pd(PPh$_3$)$_4$/CuI	25	2; 24	Filtered on Büchner Chromatography on silica gel	34
Propane-1,2-diol	Pd(PPh$_3$)$_4$/CuI	25	24	Filtered on Büchner Chromatography on silica gel	72
[a] Already described and reported for comparison. [b] Pd catalyst/CuI ratio: 1:1 (0.05 eq)					

obtained values could be further lowered when working with larger quantities. Given the generally good results obtained with aryl iodides, even those with electron-donating substituents, we decided to evaluate the effectiveness of glycerol with aryl bromides, known to be generally less reactive than iodides in these coupling reactions ever since the first studies.[28] We therefore extended the tests to the coupling between 2-bromo-3-hexylthiophene (TP-3HeT) (Scheme 3) and TETPA, and 4-tribromotriphenylamine itself, being the reaction with trimethylsilylacetylene (TMSA) the first synthetic step to obtain our products as sketched in Scheme 1. Both derivatives were intentionally chosen with electron-donating substituents, to further make the reaction more challenging. In both cases, the reactions provided moderate yields, reported in Table 2. In the case of TP-3TMSA formation, the lower yield can be attributed to the combined effects of reduced reactivity of aryl bromides and volatility of trimethylsilylacetylene at 80 °C accentuated by its poor solubility in glycerol that led to its depletion from the reaction mixture. TP-3HeT exhibits only a slight yield increase in glycerol compared to toluene, and this suggests that the lower reactivity of bromides may still be the dominant factor and aligns with established knowledge. Similar to the results observed with aryl iodides, the E-factor value for the synthesis of TP-3HeT in glycerol is lower than that in toluene. All things considered, glycerol emerges as a compelling alternative to toluene for the cross-coupling of aryl iodides with terminal alkynes in high yields. As far as bromides are concerned,
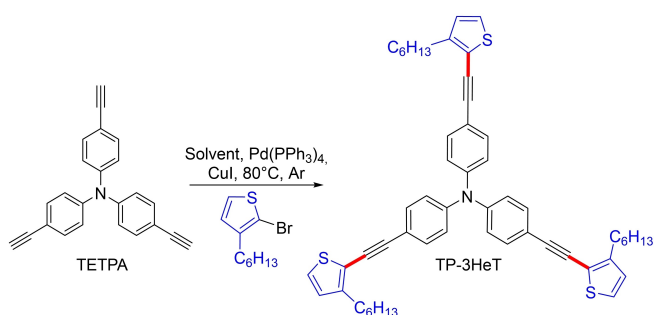
preliminary experiments suggest that the reaction is feasible, although further testing and optimization of the experimental conditions are required.

Optical Properties

The optical absorption and emission properties of the synthesized derivatives in dichloromethane (DCM) solution have been measured. All the derivatives exhibit a broad red-shifted absorption compared to the precursor tris(4-bromophenyl)amine in the near UV-visible violet region, ranging from 354 to 418 nm as shown in Figure 2, compatible with a significant extension of conjugation of all the molecules. The absorption maxima are correlated with the nature of the peripheral group. The more electron-donating the group, as in the case of TP-3EPOMe, the more blueshifted the absorption peak, whereas the more electron-withdrawing the substituent group, as in the case of TP-3BEs derivative bearing hexyl benzoate moieties, the more pronounced the bathochromic effect.

The TP-6CN derivative has the most redshifted absorption maximum in the visible region at 418 nm due to the extended electronic conjugation on its cyano groups. Steady-state fluorescence measurements in dichloromethane have been performed to evaluate the emission characteristics of the new compounds. All synthesized derivatives exhibit a Stokes shift: for D-(π-D)$_3$ derivatives, the shift is between 0.36 eV to 0.40 eV, while D-(π-A)$_3$ derivatives exhibit larger values, ranging from 0.51 eV to 0.63 eV. TP-3HeT exhibits the smallest shift, whereas TP-6CN demonstrates the largest.

Furthermore, the optical gaps of the synthesized derivatives reflect the nature of the substituents present on their periphery. This is particularly evident in the case of TP-6CN, which exhibits the lowest optical gap among all the derivatives, as also confirmed by the closest measured and calculated oxidation potentials and HOMO-LUMO frontier orbitals discussed below. This can be attributed to the high degree of electron delocalization within the molecule, allowing electrons to participate in more vibrational modes. This, in turn, contributes
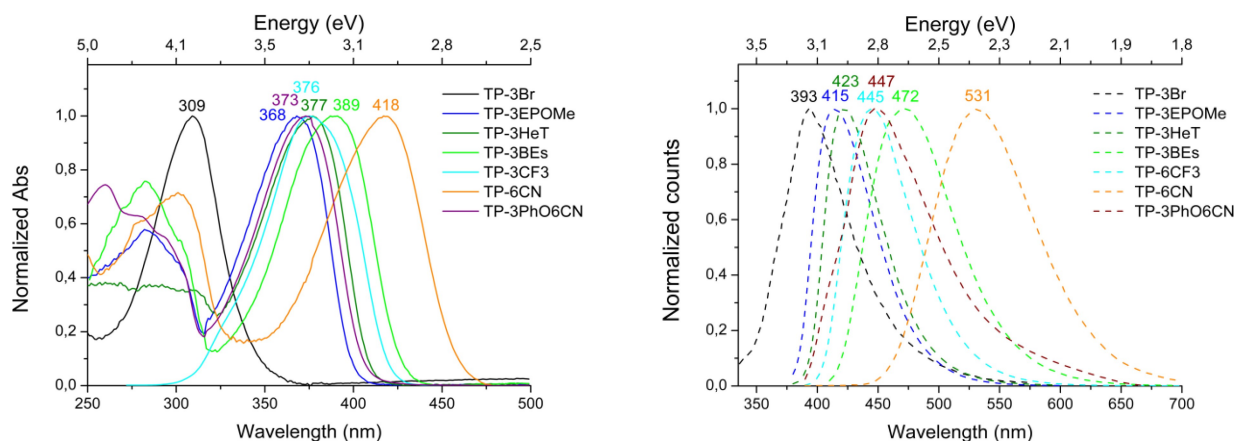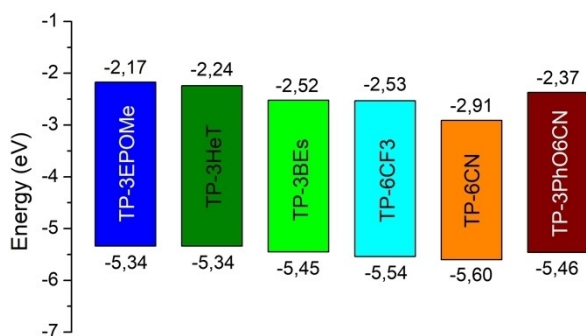

Scheme 3. General reaction conditions for the synthesis of TP-3HeT.

Figure 2. Absorption (left panel) and emission (right panel) spectra of synthesized molecules in dichloromethane solution.

Chemistry–A European Journal

Research Article
doi.org/10.1002/chem.202402901

Chemistry Europe
European Chemical
Societies Publishing

Figure 3. Voltammetric HOMO and LUMO energy levels diagram of target derivatives.

to a larger Stokes shift. Another example is the relatively low optical gap of TP-3BEs compared to the TP-3EPOMe analogous.

In this case, in addition to electron delocalization, the non-rigid nature of the excited state must also be considered. Due to the presence of a C_6H_{13} alkyl chain, this derivative can undergo more extensive vibrational relaxation, settling into a more stable configuration in the excited state. This additional relaxation pathway can lead to energy loss, manifested as a lower energy of emitted light compared to the absorbed light. All experimental optical results are summarized in Table 4. The Stokes shift values of the D-$(\pi$-A$)_3$ derivatives, combined with their limited absorption in the visible region of the solar spectrum, suggest their potential as candidates in transparent solar conversion systems such as luminescent solar concentrators, with promising applications in Building-Integrated Photovoltaics (BIPV).

Electrochemical Characterization

In addition, the electrochemical behavior of the synthesized molecules was investigated in DCM containing 0.1 M tetrabuty-lammonium hexafluorophosphate (TBAPF$_6$) in a three-electrode cell by cyclic voltammetry (CV). The obtained electrochemical data are represented in Figure 3 and summarized in Table 4, while further experimental details and CV diagrams are given in the Supporting Information. Oxidation potentials range from

−5.34 eV of TP-3EPOMe and TP-3HeT to −5.60 eV of TP-6CN as confirmed by the theoretical calculations. Based on the voltammetric measurements, TP-3EPOMe, TP-3HeT and TP-3PhO6CN have optimal oxidation values for application in photovoltaics as hole transporters. Furthermore, the presence of oxygen, sulfur and cyano groups on their structures may favor passivation of defects through Lewis acid-base interactions in the photoactive layers of photovoltaic devices, as reported in the case of perovskite-solar cells.

DFT Calculations

DFT calculations provide a powerful, complementary tool for the investigation of classes of molecules and for the prediction, often very accurate, of trends in chemical and physical properties before actual synthesis of the selected targets.

As a consequence of the C3 symmetry, all the molecules are characterized by frontier orbitals having A (HOMO) and E (degenerate LUMO) symmetry. Energies of such orbitals, calculated at the B3LYP@def2-TZVPP level of theory (see SI for an exhaustive account of theoretical methods), are shown in Figure 4 (a). An analysis of such energies confirms the idea that electron-rich substituents matching the electron donor behavior of the TPA core like TP-3EPOMe and TP-3HeT have higher HOMO levels, and higher calculated oxidation potentials, all reported in Table S3. On the other hand, the electron-acceptor substituents of TP-3BEs, TP-6CF3 and TP-6CN have a marked effect in the lowering of the corresponding LUMO levels, suggesting the shift of absorption onsets toward the visible region and the formation of charge-transfer states upon excitation. Halfway we found the interesting architecture of TP-3PhO6CN, mixing the marked donor character of -OR substituents, which raises the HOMO at the same level of TP-3HeT, with the presence of six strong -CN acceptors, which lower the LUMO closer to TP-6CN.

Indeed, time-dependent density functional theory (TDDFT) calculations shown in Figure 4 (b and c) reproduce absorption and emission spectra in dichloromethane of the six investigated molecules in good agreement with measurements, shown in Figure 2, even considering an overestimation of Stokes shifts in the case of donor substituents using the present computational setup (all numerical data are reported in Table S3). All the

Compound	λ_{abs} (nm)	λ_{em} (nm)	Stokes shift (eV)	Stokes shift (cm^{-1})	Eg$_{opt}$ (eV)	$E_{0/+}$ (eV)[a]	$E_{0/-}$ (eV)[b]
TP-3EPOMe	368	415	0.38	3078	3.17	−5.34	−2.17
TP-3HeT	377	423	0.36	2885	3.10	−5.35	−2.24
TP-3PhO6CN	373	447	0.55	4438	3.09	−5.46	−2.37
TP-3BEs	389	472	0.56	4521	2.93	−5.45	−2.52
TP-6CF3	376	445	0.51	4124	3.01	−5.54	−2.53
TP-6CN	418	531	0.63	5091	2.69	−5.60	−2.91

Table 4. Optical and electrochemical properties of target compounds.

[a] Oxidation potentials were calculated with the equation $E0_{/+} = -[(E_{ox} - E_{Fc+/Fc}) + 4.8]$. [b] Reduction potentials were estimated from the optical gap as follows: $E_{0/-}$ (eV) $= E_{0/+} + Eg_{opt}$.
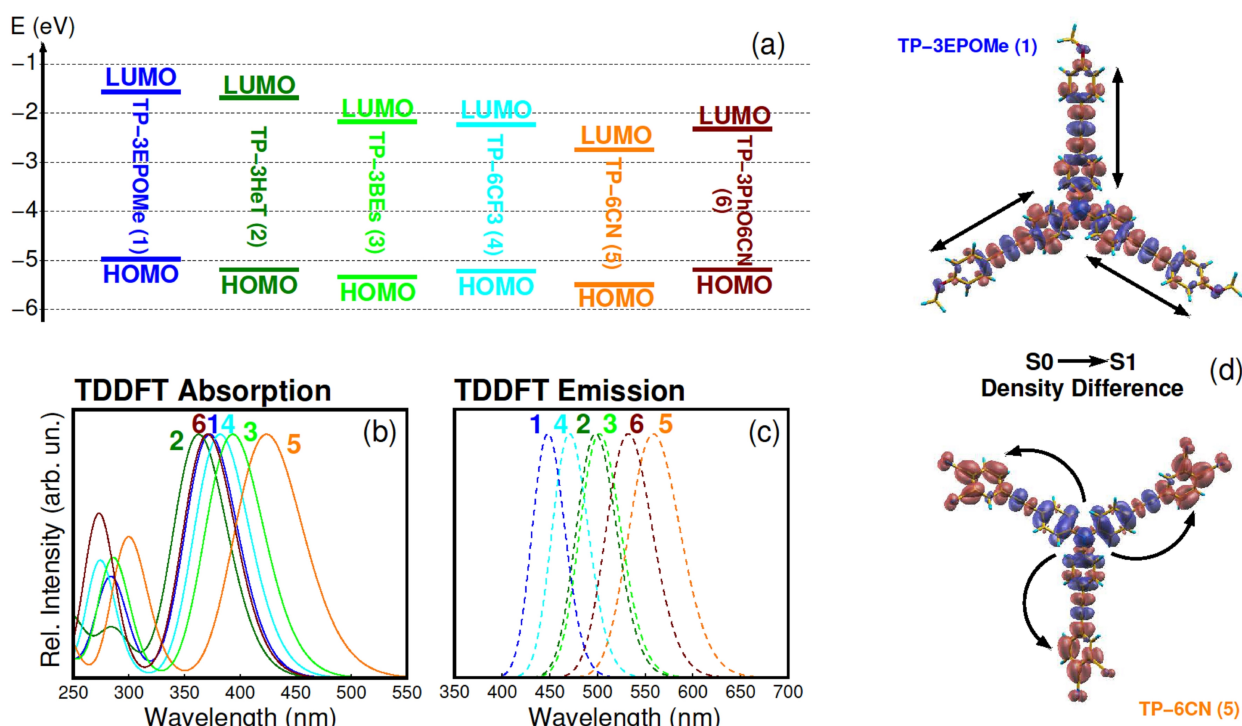
Figure 4. (a) Energy values of frontiers orbitals of TP-3EPOMe, TP-3HeT, TP-6CF3, TP-3BEs, TP-3PhO6CN and TP-6CN calculated in dichloromethane at the B3LYP@def2-TZVPP level of theory. TDDFT absorption (b) and emission (c) spectra of the same molecules. (d) TDDFT density difference maps of TP-3EPOMe (upper panel) and TP-6CN (lower panel). Charge is displaced from blue regions to red regions upon excitation of the molecules from the ground state S0 to the first excited state S1.

molecules are characterized by strong S0→S1 transitions that can be almost entirely ($>90\%$) assigned to single-particle, dipole allowed A→E transitions between HOMO and LUMO. However, displacement of charge upon excitation depends strongly on the nature of substituents. Figure 4(d) illustrates the significant difference between D-(π-A$_3$) and D-(π-D$_3$) architectures in this regard. The two maps show the difference between the charge density of the S0 ground state and the S1 first excited state, highlighting regions of charge accumulation (in red) and depletion (in blue) activated when the molecule is excited from S0 to S1. In the case of TP-6CN (lower panel), S1 is a CT state, with a clear displacement of charge from the central amino group to the peripheral phthalonitrile groups. Such a strong D-(π-A)$_3$ behavior, accompanied by a significant Stokes shift, is suitable for the use of such subclass of molecules in opto-electronic devices involving absorption-emission of light. In the case of TP-3EPOMe (upper panel), the transition to the excited state is clearly dominated by a short-range rearrangement of the charge density due to the comparable polarization of the branches in the D-(π-D)$_3$ architecture. Such optoelectronic features, accompanied by the largest HOMO-LUMO gap, make TP-3EPOMe and TP-3HeT good candidates as hole-transport and electron-blocking layers in opto-electronic devices involving charge transport.

Conclusions

This study demonstrates the successful use of glycerol as a sustainable solvent for Sonogashira cross-coupling reactions, resulting in high product yields for a series of three-legged triphenylamine derivatives. When compared to conventional organic solvents like toluene, glycerol allowed for easier product isolation and much faster reaction times. The reaction showed tolerance to a variety of functional groups, demonstrating its versatility. While the favorable effect of electron-withdrawing groups on the aryl halide reactivity was confirmed, the surprising behavior of the TP-3BEs derivative highlights the need for further investigation into the role of alkyl chain length and solvent polarity in these reactions. Moreover, propylene glycol has emerged as a potential alternative solvent, necessitating more optimization studies to further improve yields and reaction rates. Our alternative method allowed us to synthesize a varied portfolio of original molecular materials with tailored optoelectronic properties, making them promising candidates for implementation in advanced energy conversion technologies. Implementing glycerol as a solvent not only reduces the environmental impact of the reaction but also opens doors for future research in developing sustainable protocols for similar cross-coupling reactions. This work could serve as a stepping stone for designing and synthesizing novel functional materials with an emphasis on environmental responsibility.

Chemistry–A European Journal

Research Article
doi.org/10.1002/chem.202402901

Chemistry
Europe

European Chemical
Societies Publishing

Experimental Section

Materials and Methods

All reagents and solvents were purchased from Merck Life Science, TCI Chemicals, and Carlo Erba Reagents and used without further purification with the exception of tris(4-bromophenyl)amine which was recrystallized in EtOH. Reactions were monitored by thin-layer chromatography (TLC) employing a polyester layer coated with 250 mm F254 silica gel. Chromatographic purifications, when needed, were performed using silica gel 60 A 35–70. ^{1}H NMR spectra were recorded on a Bruker AVANCE 600 NMR spectrometer operating at a proton frequency of 600.13 MHz; chemical shifts (δ) are given in ppm relative to tetramethylsilane (TMS). UV-Vis spectra were recorded on a Perkin-Elmer Lambda 950 UV-vis/NIR spectrophotometer. MALDI-TOF spectra were recorded at Toscana Life Science facility in a MALDI-TOF/TOF Ultraflex III (Bruker). Melting points were determined using a Büchi 535 apparatus. Steady-state fluorescence spectra were recorded with a JobinYvon Fluorolog3 spectrofluorometer. The emissions have been collected in various ranges between 370 and 700 nm, exciting the sample with appropriate wavelengths, and 1 nm grids. No filters have been used. All experiments were performed at room temperature using quartz cuvettes with an optical path length of 10 mm. Cyclic voltammetry (CV) measurements were carried out at 25 °C with a potentiostat-galvanostat Metrohm PGStat204 in a conventional three electrodes cell. A platinum disk (~1 mm) was used as a working electrode together with a platinum wire as an auxiliary electrode. The reference electrode was Ag/AgCl and the Fc$^+$/Fc (ferrocenium/ferrocene) couple was used as an external standard. The sample solutions were ~10^{-3} M in freshly distilled dichloromethane, and dry tetrabutylammonium hexafluorophosphate (TBAPF$_6$) was used as the supporting electrolyte at 0.1 M concentration. The solutions were previously purged for 10 min with nitrogen, and all measurements were performed under an inert atmosphere. The voltammograms were recorded at scan rates ranging from 0.05 to 0.1 V s^{-1}.

General Procedure for the Synthesis of Sonogashira Coupling Derivatives in Standard Conditions [A]

The aryl halide (0.51 mmol, 3.2 eq) was dissolved in toluene (2 mL) under argon atmosphere. Then Pd(PPh$_3$)$_4$ (0.008 mmol, 0.05 eq), triethylamine (3 mL), tris(4-ethynylphenyl)amine (0.16 mmol, 1 eq), and CuI (0.008 mmol, 0.05 eq) were added. The reactions were stirred for 1 d at 80 °C. Then the reaction mixture was diluted with H$_2$O and extracted with dichloromethane in a separating funnel. Then, the organic phases were evaporated under reduced pressure. The products were purified through column chromatography with silica gel and different eluting mixtures.

General Procedure for the Synthesis of Sonogashira Coupling Derivatives in Glycerol [B]

The aryl halide (0.51 mmol, 3.2 eq) was dissolved in glycerol (2 mL) at room temperature under argon atmosphere. Then Pd(PPh$_3$)$_4$ (0.008 mmol, 0.05 eq), triethylamine (3 mL), tris(4-ethynylphenyl)amine (0.16 mmol, 1 eq), and CuI (0.008 mmol, 0.05 eq) were added. The reaction usually appeared to be over in 15 min; however, they were vigorously stirred (1000 rpm) for a few hours at 80 °C. Then the reaction mixtures were diluted with 15 mL H$_2$O, treated with 5 ml of HCl 1 N and filtered on Büchner. The products were recrystallized in dichloromethane, or in hexane/dichloromethane mixtures.

Tris(4-((3-hexylthiophen-2-yl)ethynyl)phenyl)amine (TP-3HeT)

Yield [A] 35%. [B] 42%. Transparent/light green oil. ^{1}H NMR (600 MHz, CDCl$_3$) δ 7.40 (d, $J=8.7$ Hz, 6H), 7.17 (d, $J=5.2$ Hz, 3H), 7.07 (d, $J=8.7$ Hz, 6H), 6.88 (d, $J=5.1$ Hz, 3H), 2.77–2.72 (m, 6H), 1.69–1.62 (m, 6H), 1.40–1.29 (m, 18H), 0.88 (t, $J=7.0$ Hz, 9H). ^{13}C NMR (151 MHz, CDCl$_3$) δ 147.67, 146.61, 132.52, 128.28, 125.85, 124.05, 118.42, 118.09, 95.00, 82.36, 31.66, 30.25, 29.55, 28.97, 22.63, 14.12. MALDI-TOF m/z Calcd: 815.3653 Found: 815.307.

Tris(4-((4-methoxyphenyl)ethynyl)phenyl)amine (TP-3EPOMe)

Yield [A] 96%. [B] 87%. Yellow solid. mp 131–132 °C. ^{1}H NMR (600 MHz, CDCl$_3$) δ 7.47 (d, $J=8.9$ Hz, 6H), 7.42 (d, $J=8.7$ Hz, 6H), 7.06 (d, $J=8.7$ Hz, 6H), 6.88 (d, $J=8.9$ Hz, 6H), 3.83 (s, 9H). ^{13}C NMR (151 MHz, CDCl3) δ 159.55, 146.50, 132.97, 132.61, 124.00, 118.24, 115.55, 114.02, 89.20, 87.92, 55.31. MALDI-TOF m/z Calcd: 635.2460 Found: 635.121.

Trihexyl 4,4′,4′′-((nitrilotris(benzene-4,1-diyl))tris(ethyne-2,1-diyl))tribenzoate (TP-3BEs)

Yield [A] 87%. [B] 50%. Brilliant green/yellow solid. mp 162–164 °C. ^{1}H NMR (600 MHz, CDCl$_3$) δ 8.02 (d, $J=8.5$ Hz, 6H), 7.57 (d, $J=8.5$ Hz, 6H), 7.47 (d, $J=8.7$ Hz, 6H), 7.10 (d, $J=8.7$ Hz, 6H), 4.33 (t, $J=6.7$ Hz, 6H), 1.81–1.74 (m, 6H), 1.48–1.43 (m, 6H), 1.37–1.33 (m, 12H), 0.93–0.90 (m, 9H). ^{13}C NMR (151 MHz, CDCl$_3$) δ 166.15, 146.96, 133.04, 131.36, 129.77, 129.50, 127.96, 124.11, 117.62, 92.15, 88.82, 77.24, 77.02, 76.81, 65.34, 31.47, 28.69, 25.72, 22.56, 14.01. MALDI-TOF m/z Calcd: 929.4655 Found: 929.451.

Trimethyl 4,4′,4′′-((nitrilotris(benzene-4,1-diyl))tris(ethyne-2,1-diyl))tribenzoate (TP-3COOMe)

Yield [B] 98%. Brilliant green/yellow solid. ^{1}H NMR (600 MHz, CDCl$_3$) δ 8.02 (d, J$=8.4$ Hz, 6H), 7.57 (d, J$=8.4$ Hz, 6H), 7.46 (d, J$=8.6$ Hz, 6H), 7.10 (d, J$=8.6$ Hz, 6H), 3.93 (s, 9H). ^{13}C NMR (151 MHz, CDCl$_3$) δ 166.58, 146.97, 133.04, 131.40, 129.55, 129.37, 128.10, 124.12, 117.59, 92.25, 88.76, 52.23.

Tris(4-((4-(trifluoromethyl)phenyl)ethynyl)phenyl)amine (TP-6CF3)

Yield [A] 98%. [B] 89%. Yellow solid. mp 283 °C (dec.). ^{1}H NMR (600 MHz, CDCl$_3$) δ 7.95 (s, 6H), 7.81 (s, 3H), 7.49 (d, $J=8.7$ Hz, 6H), 7.13 (d, $J=8.7$ Hz, 6H). ^{13}C NMR (151 MHz, CDCl$_3$) δ 147.26 (s), 133.21 (q, $J=18.3$ Hz), 132.00 (q, $J=33.7$ Hz), 131.30 (q, $J=21.7$ Hz), 125.70 (s), 124.23 (s), 122.98 (q, $J=273.0$ Hz), 121.41 (e), 116.91 (s), 92.60 (s), 86.52 (s). MALDI-TOF m/z Calcd: 953.1387 Found: 953.094.

4,4′,4′′-((nitrilotris(benzene-4,1-diyl))tris(ethyne-2,1-diyl))triphthalonitrile (TP-6CN)

Yield [A] 90%. [B] 94%. Dark orange solid. mp 177–180 °C. ^{1}H NMR (600 MHz, CDCl$_3$) δ 7.90 (d, J$=1.0$ Hz, 3H), 7.82–7.77 (m, 6H), 7.49 (d, J$=8.7$ Hz, 6H), 7.14 (d, J$=8.7$ Hz, 6H). ^{13}C NMR (151 MHz, CDCl$_3$) δ 147.53, 135.87, 135.37, 133.53, 133.49, 129.34, 129.05, 128.24, 125.31, 124.31, 116.53, 116.36, 115.21, 114.79, 114.10, 96.53, 86.24. MALDI-TOF m/z Calcd: 695.1858 Found: 695.075.

Chemistry–A European Journal

Research Article
doi.org/10.1002/chem.202402901

Chemistry Europe
European Chemical
Societies Publishing

4,4′,4′′-((((nitrilotris(benzene-4,1-diyl))tris(ethyne-2,1-diyl))tris(2,6-dimethylbenzene-4,1-diyl))tris(oxy))triphthalonitrile (TP-3PhO6CN)

Yield [A] 89%. [B] 91%. Red/orange solid. mp 186–190 °C. ^{1}H NMR (600 MHz, CDCl$_3$) δ 7.72 (d, $J=8.7$ Hz, 3H), 7.45 (d, $J=8.7$ Hz, 6H), 7.34 (s, 6H), 7.14 (dd, $J=19.7$, 2.5 Hz, 6H), 7.10 (d, $J=8.7$ Hz, 6H), 2.10 (s, 18H). ^{13}C NMR (151 MHz, CDCl$_3$) δ 160.79, 149.30, 146.81, 135.68, 132.88, 132.72, 130.95, 124.10, 121.88, 119.70, 119.56, 118.02, 117.79, 115.33, 114.92, 108.73, 89.64, 88.26, 16.07. MALDI-TOF m/z Calcd: 1055.3584 Found: 1055.353.

Atomistic Simulations

Atomistic simulations of the six molecules TP-3EPOMe, TP-3HeT, TP-6CF3, TP-3BEs TP-3PhO6CN and TP-6CN have been performed using a multi-level protocol. The most stable conformers of the molecules have been individuated by a conformer-rotamer ensemble sampling tool (CREST) algorithm,[29] which uses the tight-binding GFN2-xTB Hamiltonian as "engine" for the search of minimum energy configurations.[30] Electronic and optical properties of the most stable conformers have been then investigated using (time-dependent) density functional theory simulations, carried out in a GTO framework using the ORCA suite of programs.[31] A detailed description of theoretical methods is provided in the Supporting Information.

Supporting Information Summary

The Supporting Information includes all the detailed synthetic procedures, with E-factor calculations and cost estimation for each derivative. Additionally, it contains ^{1}H, ^{13}C NMR and MALDI-TOF spectra, cyclic voltammograms, and detailed atomistic simulations. The authors have cited additional references within the Supporting Information.[32–37]

Conflict of Interests

The authors declare no conflict of interest.

Data Availability Statement

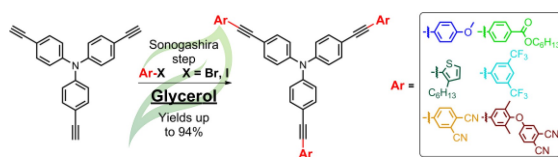The data that support the findings of this study are available in the supplementary material of this article.

Keywords: Sonogashira reaction · Sustainable chemistry · Green solvents · Organic functional materials · C—C coupling

[1] P. Anastas, N. Eghbali, *Chem. Soc. Rev.* **2010**, *39*, 301–312.

[2] R. A. Sheldon, *Green Chem.* **2005**, *7*, 267–278.

[3] Y. Hayashi, *Chem. Sci.* **2016**, *7*, 866–880.

[4] C. O. Kappe, *Angew. Chem. Int. Ed.* **2004**, *43*, 6250–6284.

[5] O. Ostroverkhova, *Handbook of Organic Materials for Optical and (Opto)Electronic Devices: Properties and Applications*, Woodhead Publishing, Philadelphia, **2013**, 3–82.

[6] a) A. Pron, R. R. Reghu, R. Rybakiewicz, H. Cybulski, D. Djurado, J. V. Grazulevicius, M. Zagorska, I. Kulszewicz-Bajer, J.-M. Verilhac *J. Phys. Chem. C.* **2011**, *115*(30), 15008–15017; b) P. Devibala, B. Balambiga, P. M. Imranb, S. Nagarajan, *New J. Chem.* **2024**, *48*, 193–202.

[7] a) O. Bezvikonnyi, R. Durgaryan, T. Tamulevicius, D. Volyniuk, A. Jurkeviciute, J. Simokaitiene, Y. Danyliv, S. Vardanyan, S. Macionis, J. V, Grazulevicius, *Spectrochim. Acta A Mol. Biomol. Spectrosc.* **2024**, *321*, 124713; b) P. Cias, C. Slugovc, G. Gescheidt, *J. Phys. Chem. A.* **2011**, *115*(50), 14519–14525; c) A. Degli Esposti, V. Fattori, C. Sabatini, G. Casalbore-Miceli, G. Marconi, *Phys. Chem. Chem. Phys.* **2005**, *7*, 3738–3743.

[8] J. Wang, K. Liu, L. Ma, X. Zhan, *Chem. Rev.* **2016**, *116*, 14675–14725.

[9] M. Klikar, P. Solanke, J. Tydlitát, *Chem. Rec.* **2016**, *16*, 1886–905.

[10] a) J. Wang, K. Liu, L. Ma, X. Zhan, *Chem. Rev.* **2016**, *116*(23), 14675–14725; b) R. Fuentes Pineda, Y. Zems, J. Troughton, M. R. Niazi, D. F. Perepichka, T. Watson, N. Robertson, *Sustain. Energy Fuels.* **2020**, *4*(2), 779–787.

[11] H. U. Kim, T. Kim, C. Kim, M. Kim, T. Park, *Adv. Funct. Mater.* **2023**, *33*, 2208082.

[12] A. Abate, M. Planells, D. J. Hollman, V. Barthi, S. Chand, H. J. Snaith, N. Robertson, *Phys. Chem. Chem. Phys.* **2015**, *17*, 2335–2338.

[13] A. Soheili, J. Albaneze-Walker, J. A. Murry, P. G. Dormer, D. L. Hughes, *Org. Lett.* **2003**, *5*(22), 4191–4194.

[14] a) Y. Tian, J. Wang, X. Cheng, K. Liu, T. Wu, X. Qiu, Z. Kuang, Z. Li, J. Bian, *Green Chem.* **2020**, *22*, 1338–1344; b) E. Ghiglietti, E. A. Incarbone, S. Mattiello, L. Beverina, *Eur. J. Org. Chem.* **2024**, *27*, e202400223.

[15] B. H. Lipshutz, D. W. Chung, B. Rich, *Org. Lett.* **2008**, *10*(17), 3793–3796.

[16] J. Struwe, L. Ackermann, F. Gallou, *Chem. Catal.* **2023**, *3*, 100485.

[17] P. S. Kong, M. K. Aroua, W. M. Ashri, W. Daud, *Renew. Sustain. Energy Rev.* **2016**, *63*, 533–555.

[18] A. Wolfson, C. Dlugy, Y. Shotland, *Environ. Chem. Lett.* **2007**, *5*, 67–71.

[19] J. I. García, H. García-Marína, *Green Chem.* **2014**, *16*, 1007–1033.

[20] F. Messa, G. Dilauro, F. M. Perna, P. Vitale, V. Capriati, A. Salomone, *ChemCatChem.* **2020**, *12*, 1979–1984.

[21] P. Adler, T. P.-A. Dumas, E. Deyris, *J. Clean. Prod.* **2021**, *293*, 126164.

[22] a) A. Wolfson, C. Dlugy *Chem. Pap.* **2007**, *61*(3), 228–232; b) G. Cravotto, L. Orio, E. Calcio Gaudino, K. Martina, D. Tavor, A. Wolfson, *ChemSusChem.* **2011**, *4*, 1130–1134; c) G. Clavé, F. Pelissier, S. Campidelli, C. Grison, *Green Chem.* **2017**, *19*, 4093–4103.

[23] Z. Zhikai, W. Qing, L. Haiming, L. Tao, R. Yi, *J. Am. Chem. Soc.* **2022**, *144*(26), 11748–11756.

[24] a) M. García-Melchor, M. C. Pacheco, C. Nájera, A. Lledós, G. Ujaque, *ACS Catal.* **2012**, *2*(1), 135–144; b) C. He, J. Ke, H. Xu, A. Lei, *Angew. Chem., Int. Ed.* **2013**, *52*, 1527–1530; c) R. Chinchilla, C. Nájera, *Chem. Rev.* **2007**, *107*(3), 874–922.

[25] C. A. Fleckenstein, H. Plenio, *Chem. Soc. Rev.* **2010**, *39*, 694–711.

[26] J. F. Hartwig, *Inorg. Chem.* **2007**, *46*, 1936–1947.

[27] T. P. Osedach, T. L Andrew, V. Bulović *Energy Environ. Sci.* **2013**, *6*, 711–718.

[28] E. Negishi, L. Anastasia, *Chem. Rev.* **2003**, *103*(5), 1979–2018.

[29] P. Pracht, F. Bohle, S. Grimme, *Phys. Chem. Chem. Phys.* **2020**, *22*, 7169–7192.

[30] a) C. Bannwarth, S. Ehlert, S. Grimme, *J. Chem. Theory Comput.* **2019**, *15*, 1652–1671; b) S. Grimme, *J. Chem. Theory Comput.* **2019**, *15*, 2847–2862.

[31] a) F. Neese, *Wiley Interdiscip. Rev. Comput. Mol. Sci.* **2012**, *2*, 73–78; b) F. Neese, *Wiley Interdiscip. Rev. Comput. Mol. Sci.* **2018**, *8*, e1327.

Chemistry–A European Journal

Research Article
doi.org/10.1002/chem.202402901

Chemistry Europe
European Chemical
Societies Publishing

[32] a) A. Schäfer, H. Horn, R. Ahlrichs, *J. Chem. Phys.* **1992**, *97*, 2571–2577; b) F. Weigend, R. Ahlrichs, *Phys. Chem. Chem. Phys.* **2005**, *7*, 3297–3305.

[33] V. Barone, M. Cossi, *J. Phys. Chem. A.* **1998**, *102*, 1995–2001.

[34] A. D. Becke, *J. Chem. Phys.* **1992**, *96*, 2155–2160.

[35] E. Caldeweyher, C. Bannwarth, S. Grimme, *J. Chem. Phys.* **2017**, *147*, 034112.

[36] Y. Zhang, W. Yang, *Phys. Rev. Lett.* **1998**, *80*, 890.

[37] B. De Souza, F. Neese, R. Izsák, *J. Chem. Phys.* **2018**, *148*, 034104.

RESEARCH ARTICLE

V. Raglione, F. Palmeri, G. Mattioli, F. Porcelli, D. Caschera, G. Zanotti*

1 – 11

Glycerol as Reaction Medium for Sonogashira Couplings: A Green Approach for the Synthesis of New Triarylamine-Based Materials with Potential Application in Optoelectronics

In this paper, we present an innovative method using glycerol as a green solvent for Sonogashira reactions, achieving high yields for the synthesis of triphenylamine derivatives. Compared to traditional organic solvents, glycerol accelerates reaction times and simplifies product purification. This versatile approach tolerates diverse functional groups opening new avenues for sustainable syntheses of functional materials with potential applications in optoelectronics.